

# Theoretical Study of Intermolecular Interaction at the Lipid–Water Interface. 1. Quantum Chemical Analysis Using a Reaction Field Theory

Minoru Sakurai,<sup>\*,†</sup> Hirohisa Tamagawa,<sup>†</sup> Yoshio Inoue,<sup>†</sup> Katsuhiko Ariga,<sup>‡</sup> and Toyoki Kunitake<sup>‡</sup>

Department of Biomolecular Engineering, Tokyo Institute of Technology, 4259 Nagatsuta-cho, Midori-ku, Yokohama 226, Japan, and Supermolecules Project, Japan Science and Technology Corporation (JST), Kurume Research Center Building, 2432 Aikawa-cho, Kurume, Fukuoka 839, Japan

Received: December 26, 1996; In Final Form: March 25, 1997<sup>⊗</sup>

Reaction field calculation combined with the AM1 molecular orbital method is applied in order to understand why intermolecular hydrogen bonding is stabilized at the lipid–water interface. Here, we focus on the interaction between a guanidinium-functionalized lipid (**1**) and phosphate and between a diaminotriazine-functionalized lipid (**2**) and thymine. The interface is approximated by a double layer composed of two dielectrics. The lower dielectric medium with a dielectric constant of 2 corresponds to the lipid layer, and the higher dielectric medium with dielectric constant of 80 to the aqueous subphase. A pair of interacting molecules is placed on/near the interface, and the binding energy profile is obtained. For comparison, the calculation of binding energy is also performed for a homogeneous system defined as a single dielectric constant, corresponding to a normal solution system. It is shown that the calculation reproduces well the observed binding constants, when the position of the interface is appropriately displaced relative to the interacting molecules. One of the most important findings is that hydrogen bonding is remarkably strengthened even if the binding site is exposed to the aqueous subphase. The results for the binding profiles are interpreted from those for Mulliken population analysis.

## Introduction

Hydrogen bonding drives intermolecular association in biological systems such as enzyme–substrate and antibody–antigen. Precise molecular recognition in these systems is caused by stereospecific pairing between hydrogen donor and acceptor. Recently, intensive effort has been made to realize molecular recognition through complementary hydrogen bonding in biomimetic host–guest systems.<sup>1–18</sup> However, hydrogen bonding contributes only modestly to the free energy of association of small, uncharged solute molecules in aqueous solution. Realization of effective hydrogen bonding in water is a major focus in current host–guest chemistry.

A major breakthrough in this field has been brought about by Kunitake's group. They have indicated that hydrogen bonding is remarkably enhanced at the lipid (or air)–water interface, formed by a self-assembly of amphiphiles expanded on pure water.<sup>1,12,17,18</sup> In the use of a guanidinium-functionalized monolayer, ATP (or AMP), dissolved in the aqueous subphase, binds to the guanidinium group(s) of **1** with a binding constant about  $10^6$  times larger<sup>11,12,17</sup> than the value ( $1.3 \text{ M}^{-1}$ )<sup>19</sup> for the complex of free guanidinium cations with free phosphate anions in water. Similarly, using a monolayer formed by diaminotriazine-functionalized amphiphile **2**, complementary hydrogen bonding as found between nucleic acid bases was shown to occur with the same magnitude of binding constant as in chloroform.<sup>18</sup> Molecular recognition systems using these monolayer assemblies are important in applications such as chemical sensors and in understanding molecular interactions on biological cell surfaces. In spite of such technological and scientific interests, how the intermolecular binding energy is amplified at the lipid–water interface remains to be solved.

The multiple nature of interactions between lipid molecules and substrates may contribute to the amplification of binding energy. For example, in the amphiphile **1**–ATP system mentioned above, one ATP molecule is thought to bind to three molecules of **1** at the interface. However, the effect of such multiple bonding alone is insufficient to completely explain the observed results, because the binding constant ( $1.7 \times 10^7 \text{ M}^{-1}$ ) between **1** and ATP is close to that ( $3.2 \times 10^6$ ) between **1** and AMP, where a 1:1 complex is formed.<sup>11,12,17</sup> The major part of the enhancement ( $10^6$  times) in binding constant, on going from the aqueous medium to the interface, must arise from other factors.

At present there may be a limited number of experimental techniques available to provide information on molecular interaction occurring in the interfacial environment, which means a region of  $\sim 10 \text{ \AA}$  apart from the interface. Instead, a variety of computational approaches would be possible. However, the method to be used must be able to explicitly obtain the energy profile of hydrogen bonding under the presence of interfacial effects.

Recently, we have developed a reaction field theory applicable to solvation occurring in electrostatically heterogeneous environments.<sup>20,21</sup> The theory combined with molecular orbital methods has been successfully applied to the interpretation of catalytic reaction<sup>22</sup> and <sup>13</sup>C-NMR chemical shifts of guest molecules bound to cyclodextrin (CD),<sup>23</sup> which is a representative macrocyclic host possessing a hydrophobic cavity. On complexation with CD, benzene derivatives with polar group(s), typical guest molecules, are placed at the interface formed by the CD cavity and the surrounding aqueous medium. Then, the polar group (reactive site) of the guest is located on the side of the aqueous medium and the aromatic ring is included in the hydrophobic cavity. In those studies, we have indicated that the electronic structure of the polar group is greatly influenced by a reaction field generated from the cavity, resulting

\* Author to whom all correspondence should be addressed.

<sup>†</sup> Tokyo Institute of Technology.

<sup>‡</sup> Japan Science and Technology Corporation (JST).

<sup>⊗</sup> Abstract published in *Advance ACS Abstracts*, May 1, 1997.

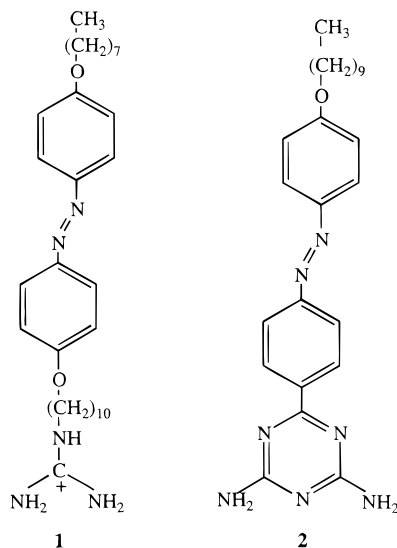


**Figure 1.** (1) Guandinium-functionalized lipid. (2) Diaminotriazine-functionalized lipid.

in a drastic change in the reaction rate of the guest. The interaction of **1** with ATP (or **2** with nucleic acid base) should occur at the interface between the hydrophobic lipid layer and the aqueous subphase. In this regard, the situation is similar to that of the CD–guest complex, which is a major motivation of the present study.

In this paper, we will apply the above theoretical methodology to the problem of anomalous intermolecular binding at the monolayer–water interface. Our main concern is addressed at obtaining a conceptual framework for an understanding of the interfacial phenomena, rather than to obtain the quantitatively exact solution. Here, we use a highly simplified model of an interacting **1**(or **2**)–substrate system at the monolayer–water interface. The interface is approximated by an electric double layer constructed from two dielectrics with different dielectric constants. A pair of interacting molecules, that is, **1**–ATP(or AMP) or **2**–thymine complex, is placed on the interface, and then the binding energy profile is obtained. The results are compared with those for the binding profile in the normal (homogeneous) solution phase. On the basis of these results, we will successfully interpret the fact that the intermolecular binding is drastically amplified at the lipid–water interface.

### Model Building

Amphiphiles **1** and **2** both possess long hydrophobic chains, as shown in Figure 1. The monolayers used in refs 11, 12, 17, and 18 are condensed, highly ordered assemblies of these lipids, which has been confirmed by the pressure–area ( $\pi$ – $A$ ) isotherms. Thus, the lipid layer should form a well-defined hydrophobic region which could be regarded as a continuum with a low dielectric constant. In this study, the exact value of the dielectric constant is not necessarily required, because the major purpose is to examine how the electrostatic heterogeneity near the interface influences the binding profile of molecules. Thus, the dielectric constant  $\epsilon$  of the lipid layer was assumed to be equal to that (nearly 2) of *n*-alkane. With the same level of approximation, the aqueous subphase could be regarded as a continuum with a dielectric constant of 80. Consequently, the lipid–water interface is represented by a double layer, where the boundary surface is assumed to be infinitely extended. A pair of interacting lipid–substrate was placed near/on the interface. The molecular axis of the complex was parallel to the monolayer normal, and its position is displaced from the interface as shown in Figures 2 and 3.

For comparison, another model was built in which the complex is embedded in a homogeneous dielectric with a dielectric constant of  $\epsilon$ . This corresponds to a normal solution phase.

In both types of models, the complex is accommodated into a cavity whose shape is taken to be interlocking van der Waals spheres located at atomic centers. The dielectric constant inside the cavity was taken to be 1. Here, we used model compounds representing only the reactive sites of actual lipid–substrate complexes. The **1**–AMP(or ATP) complex is represented by the model compound composed of a guanidinium cation with an ethyl group and a phosphate anion (Figure 2). Hereafter this model will be called the ion complex. Figure 3 shows the model compound of the **2**–nucleic acid base complex, which is called the neutral complex. These reactive site models were explicitly treated with quantum mechanics.

### Calculation

To represent the double-layer model in numerical calculations, we first considered a multidielectric system as shown in Figure 4, where a cylindrically shaped dielectric with a dielectric constant of 2 is embedded in the infinitely extended dielectric with a dielectric constant of 80. The radius and depth of the cylinder are  $r$  and  $h$  Å, respectively. The complex is placed on the interface formed between the bottom surface ( $S_1$ ) of the cylinder and the surrounding dielectric. The free energy of the whole system was calculated using the reaction field theory developed by our group.<sup>20,21</sup> The computational details for the cylinder model have already been described in ref 22.

In numerical calculation, one cannot treat an infinite size of boundary. Then, we examined the dependence of the free energy of the whole system on the cylinder size parameters,  $r$  and  $h$ . The results are shown in Figure 5, where the free energy in the case of the ion complex, placed on the interface  $C$  (Figure 2), is plotted against  $r$  or  $h$ . As can be seen from Figures 5a,b, the free energy curves against  $r$  and  $h$  begin to be saturated near 5.0 and 9.0 Å, respectively. On the basis of these results, the boundary effect generated from the bottom surface  $S_2$  and the side surface  $S_3$  of the cylinder would be nearly negligible if the values of  $r$  and  $h$  are taken to be 8.0 and 10.0 Å, respectively. These values were used for all the calculations of the ion and neutral complexes in each double-layer model.

The binding energy profile of the complex in the dielectric media was obtained by plotting the free energy of the whole system against the parameter  $R$  measuring the distance between the lipid site and the substrate. The definitions of  $R$  are shown in Figure 6. According to the atom numbering indicated in Figure 6, the parameters  $R$  for the ion and neutral complexes are the distances between C4 and P10 and between N5 and H12, respectively.

The other geometrical parameters of both complexes were determined by separately optimizing their constituent species in vacuo.<sup>24</sup> In the ion complex, the atoms H1, N2, N6, and H7 were placed on the same plane, since they are directly related to formation of hydrogen bonds. And the N2–H1(N6–H7) bond of the guanidinium group was oriented toward the nonprotonated oxygen O9(O11) of the phosphate, so as to acquire the maximal stabilization via hydrogen bonding. In the neutral complex, the two six-membered rings are placed on the same plane, and they are oriented so as to form three hydrogen bonds of N2–H1...O10, N5...H12–N13, and N8–H9...O14. All the molecular orbital calculations were performed under the AM1 approximation.<sup>25</sup>

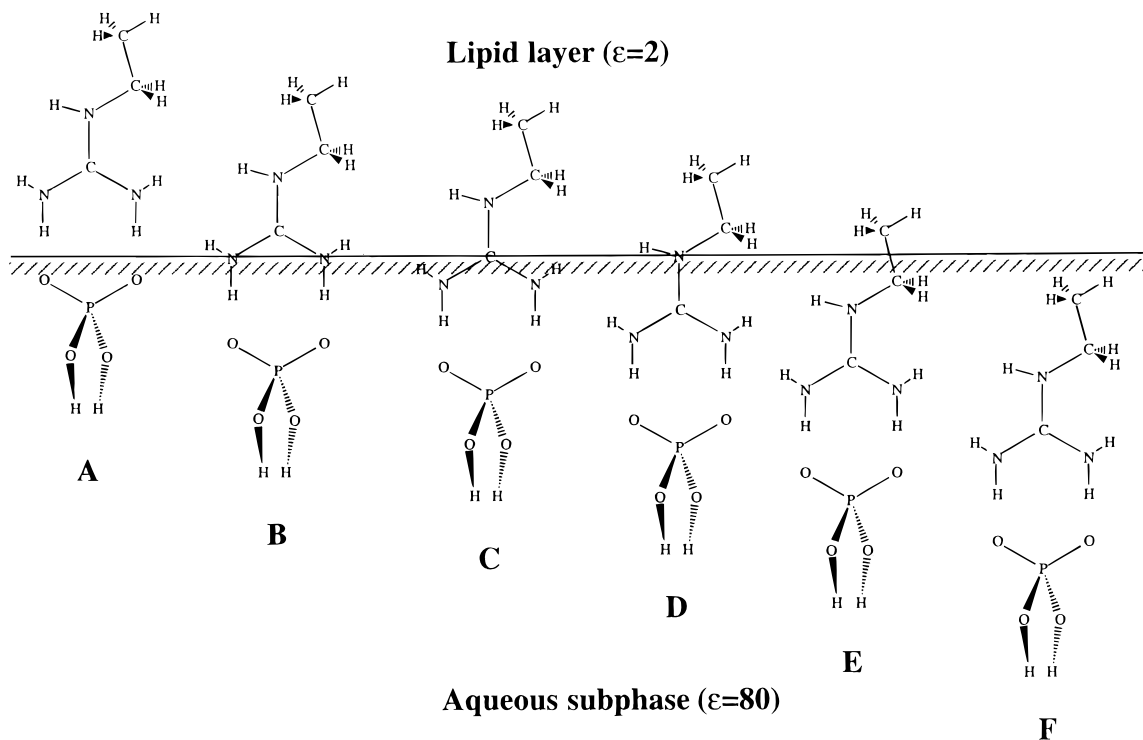


**Figure 2.** Displacement of the ion complex from the lipid–water interface.

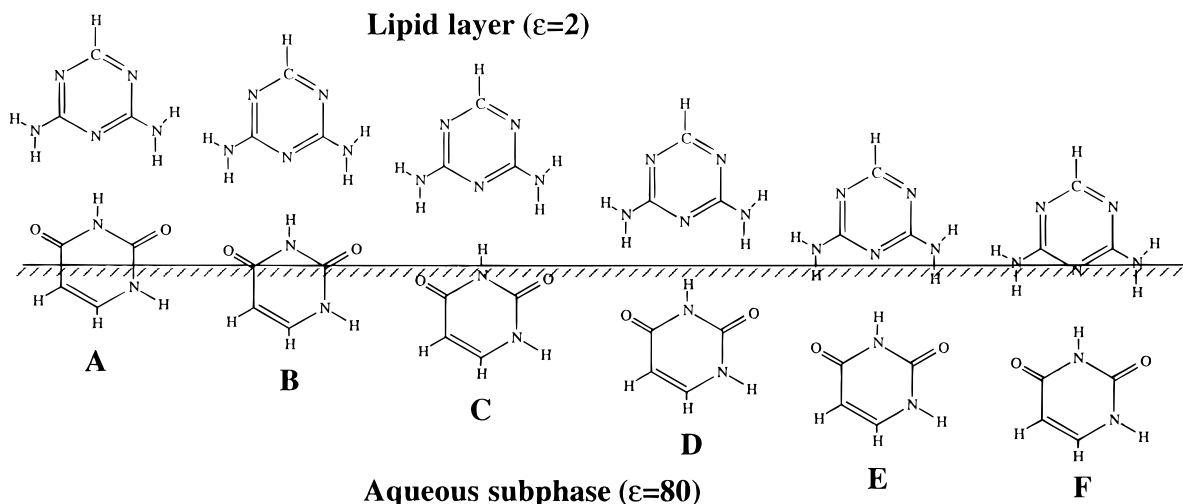


**Figure 3.** Displacement of the neutral complex from the lipid–water interface.

## Results

**Complexation in Homogeneous Media** First, in order to check the accuracy and reliability of the reaction field method used here, we examined the binding energy profile in normal liquid solution. Figure 7 shows the dependence of the free energy of the ion complex–solvent system on the distance  $R$ . In low dielectric media ( $\epsilon = 1$ –10), the potential minima are located around  $R = 4.4$  Å, indicating that the ion complex can be formed. With an increase in dielectric constant, the potential well becomes shallow and eventually disappears in the medium with a dielectric constant of 80, corresponding to the aqueous solution.

According to experimental measurements, the binding energy between the guanidinium cation and phosphate anion is  $0.78 \text{ kJ mol}^{-1}$  in water, corresponding to a binding constant of  $1.37 \text{ M}^{-1}$ .<sup>19</sup> This means that the complex and its dissociated species are populated at a ratio of 1:1 in water. The observed binding energy is considerably smaller than the thermal energy ( $RT = 2.479 \text{ kJ mol}^{-1}$ ) at room temperature. Considering these facts,

we can conclude that the calculation reproduces well the available experimental data.

The calculated binding energies are summarized in Table 1. These values were obtained by subtracting the free energy at the potential minimum from that at  $R = 30$  Å. A feature to be noted is that the binding energy depends nonlinearly on the solvent dielectric constant: a steep change occurs in a range of  $\epsilon$  from 1 to 5.

Figure 8 shows the binding energy profile of the neutral complex in solution. Similar to the case of the ion complex, the complex is formed in low dielectric media ( $\epsilon = 1$ –10): the potential minima are located near  $R = 2.2$  Å. The calculated binding energies are summarized in Table 2. These values were obtained by subtracting the free energy at the potential minimum from that at  $R = 3.8$  Å. It has been reported that the binding constant between 1-butylthymidine with pyridinediamide receptors, similar to the neutral complex used here, is  $2 \times 10^2 \text{ M}^{-1}$  in chloroform ( $\epsilon = 5$ ), corresponding to a binding energy of  $13 \text{ kJ mol}^{-1}$ .<sup>18</sup> As shown in Table 2, the calculated binding energy

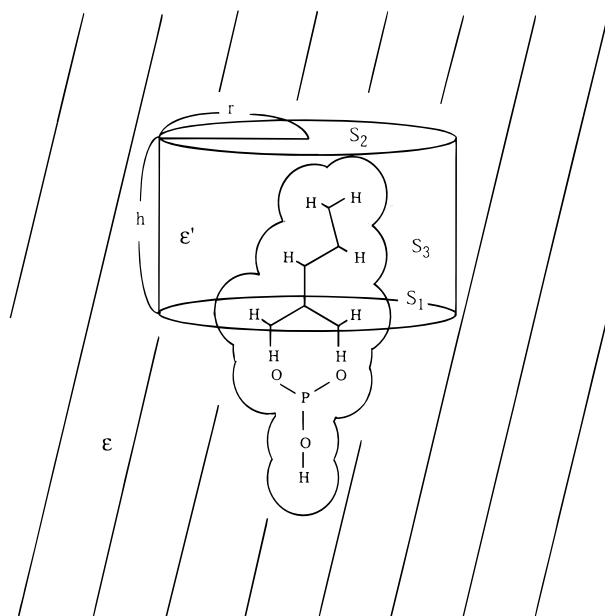


**Figure 4.** Multidielectric model used for approximately expressing the lipid–water interface. A cylindrically-shaped dielectric with a dielectric constant of 2 corresponds to the lipid phase. The cylinder is embedded in the infinitely extended dielectric with a dielectric constant  $\epsilon$  of 80, corresponding to the aqueous medium. In this example, the ion complex is located on the bottom surface  $S_1$ . The complex is accommodated into the cavity with a shape similar to its CPK model, and the inner region of the cavity has a dielectric constant of 1.

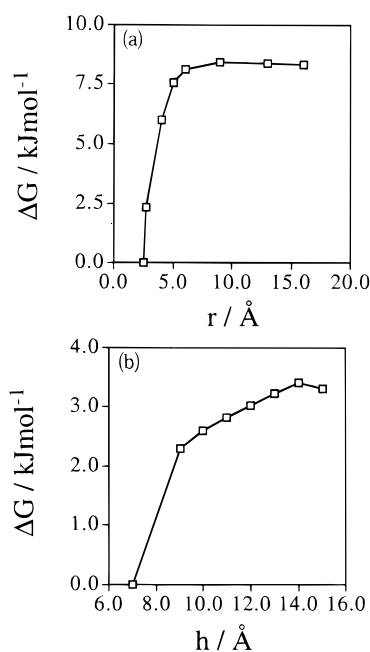


**Figure 5.** Dependence of the free energy on the cylinder size parameters,  $r$  and  $h$  given in Figure 3. (a) Free energy plotted against the radius  $r$  of the cylinder (b) Free energy plotted against the height  $h$  of the cylinder.

at  $\epsilon = 5$  is nearly zero, although the shallow potential minimum can be found near  $R = 2.2 \text{ \AA}$  (Figure 8). In the medium with a dielectric constant of 2, the binding energy is  $12.8 \text{ kJ mol}^{-1}$ . Thus, the calculation is thought to somewhat underestimate the binding energy of the neutral complex.

**Complexation on/near the Interface** The binding energy profile of each complex was obtained for several cases differing in the displacement of its reactive site from the interface. As shown in Figures 2 and 3, the complexes were gradually shifted from the lipid phase to the water phase. Hereafter, each case

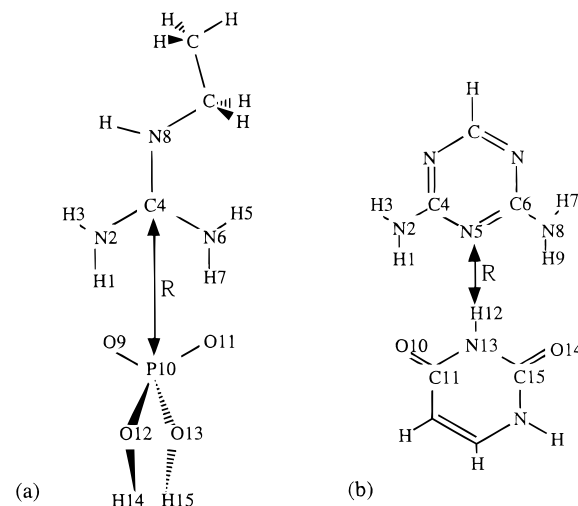


**Figure 6.** Numbering of atoms and the definition of the parameter  $R$ . (a) Ion complex, where  $R$  is the distance between C4 and P10. (b) Neutral complex, where  $R$  is the distance between C5 and H12.

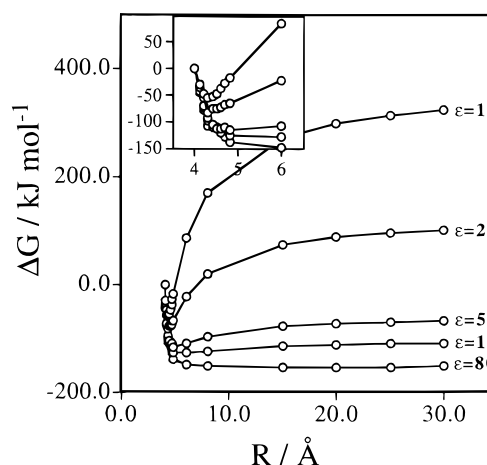


**Figure 7.** Dependence of the free energy of the ion complex–solvent system on the distance  $R$ .

**TABLE 1: Calculated and Observed Data for the Binding Energy of the Ion Complex in the Homogeneous Medium and at the Lipid–Water Interface**

$\epsilon^a$	$\Delta G_{\text{homo}}^b$	interface <sup>c</sup>	$\Delta G_{\text{int}}^d$
1	268.7	A	113.4
2	184.8	B	78.1
5	48.6	C	34.2
10	18.5	D	27.2
80	0.0	E	1.6
		F	0.0
observed	13 <sup>e</sup>		34 <sup>f</sup>

<sup>a</sup> Dielectric constant of the homogeneous medium. <sup>b</sup> Binding energy ( $\text{kJ mol}^{-1}$ ) in the homogeneous medium. <sup>c</sup> The interface position indicated in Figure 2. <sup>d</sup> The binding energy at the lipid–water interface. <sup>e</sup> Cited from ref 19. The experimental binding energy between the guanidinium cation and phosphate anion in aqueous solution. <sup>f</sup> Cited from ref 12. The experimental binding energy between the guanidinium-functionalized monolayer and AMP at the lipid–water interface.

is called interface A, B, C, and so on. For a given displacement, the free energies of the complex–double-layer systems were plotted as a function of the distance  $R$ .

Figure 9 shows the results for the ion complex. On going from interface A to F, the potential minimum becomes shallow. The binding energies are summarized in Table 1. These data were obtained in the same way as the case of homogeneous solution. In any case of interfaces A–E, the binding energy

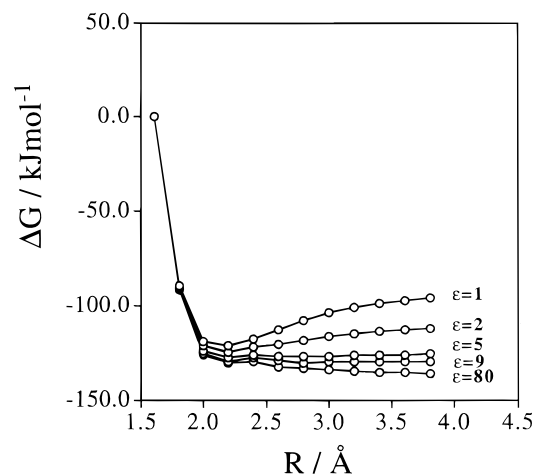


**Figure 8.** Dependence of the free energy of the neutral complex-solvent system on the distance  $R$ .

**TABLE 2: Calculated and Observed Data for Binding Energy of the Neutral Complex in the Homogeneous Medium and at the Lipid-Water Interface**

$\epsilon^a$	$\Delta G_{\text{homo}}^b$	interface <sup>c</sup>	$\Delta G_{\text{int}}^d$
1	25.2	A	11.7
2	12.8	B	10.0
5	0.0	C	8.4
9	0.0	D	0.0
80	0.0	E	0.0
		F	0.0
observed	13 <sup>e</sup>		13 <sup>f</sup>

<sup>a</sup> Dielectric constant of the homogeneous medium. <sup>b</sup> Binding energy ( $\text{kJ mol}^{-1}$ ) in the homogeneous medium. <sup>c</sup> The interface position indicated in Figure 3. <sup>d</sup> The binding energy at the lipid-water interface. <sup>e</sup> Cited from ref 18. The experimental binding energy between the 1-butylthymidine and pyridinediamide pair in  $\text{CDCl}_3$ . <sup>f</sup> Cited from ref 18. The experimental binding energy between the diaminotriazine-functionalized molecule and thymine at the lipid-water interface.

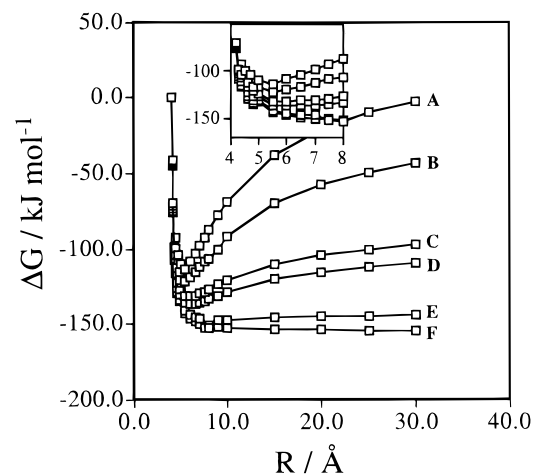


**Figure 9.** Dependence of the free energy of the ionic complex-double-layer systems on the distance  $R$ .

falls between the value ( $184.8 \text{ kJ mol}^{-1}$ ) for the homogeneous medium of  $\epsilon = 2$  and that ( $\sim 0 \text{ kJ mol}^{-1}$ ) for the medium of  $\epsilon = 80$ . The binding energy is nearly zero in the case of interface F, where the ion complex is wholly exposed to the aqueous phase. These results are naturally understood considering the features of the model used.

Surprisingly, the ion complex can be stabilized even when the binding sites, H1-O9 and H7-O11, are exposed to the aqueous phase, corresponding to interfaces B-D. It should be noted that the calculated binding energy ( $34.2 \text{ kJ mol}^{-1}$ ) is in

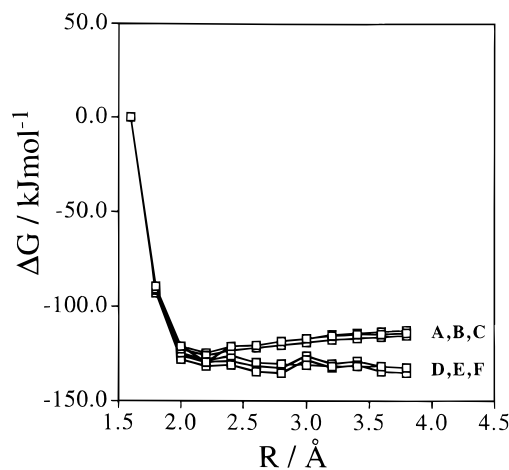


**Figure 10.** Dependence of the free energy of the neutral complex-double-layer systems on the distance  $R$ .

good agreement with the experimental data ( $34 \text{ kJ mol}^{-1}$ )<sup>11,12,17</sup> for the 1-AMP complex at the interface. According to recent molecular dynamics studies of lipid bilayer-water systems, water molecules are populated around the polar head group of the lipid, but do not penetrate into the hydrophobic phase formed by the assembly of the aliphatic chains.<sup>26-28</sup> In addition, the binding measurements for the 1-ATP system have been performed using the well-condensed, highly ordered monolayer of **1**.<sup>11,12</sup> Considering these facts, interface C is probably most reasonable among the interface positions studied here, because the hydrophobic and hydrophilic moieties of the complex are placed on the low and high dielectric phases, respectively. It can be, thus, said that the current double-layer model reproduces the essential aspect of the actual system.

Figure 10 shows the dependence of the binding energy profile of the neutral complex on the displacement of the interface. The interface positions selected are shown in Figure 3. Table 2 lists the binding energies, which was also obtained in the same way as the case of homogeneous solution. Irrespective of the positions of interface, the binding energy falls between the value ( $25.1 \text{ kJ mol}^{-1}$ ) for the homogeneous medium of  $\epsilon = 2$  and that ( $\sim 0 \text{ kJ mol}^{-1}$ ) for the medium of  $\epsilon = 80$ . Thus, the results for the double-layer model are also consistent with those for the homogeneous dielectric model. In the cases of interfaces A-C, the neutral complex can be formed, while in the other cases the complex is dissociated. In particular, it should be noted that in interface C the complex can be formed, despite the fact that the two carbonyl oxygen atoms of thymine, contributing to hydrogen bonding with the head group of **2**, are exposed to the aqueous phase. This is quite similar to the case of the ion complex with interface C or D. The binding energy of the neutral complex with interface C is  $8.4 \text{ kJ mol}^{-1}$ . On the other hand, it has been reported that the binding energy between **2** and thymine is  $13 \text{ kJ mol}^{-1}$  at the monolayer-water interface.<sup>18</sup> As described above, the reaction field theory used here tends to underestimate the binding energy of the neutral complex. Considering these facts, it can also be said that the calculated results are consistent with the experimental data. At a first glance, the interface position (interface C) capable of reproducing the experimental data seems to be excessively shifted toward the thymine moiety when compared with that (interface C) for the ion complex. However, this shift may be reasonable because the thymine ring possesses a hydrophobic moiety ( $-\text{CH}=\text{CH}-$ ) and thereby does lower polarity more than the phosphate moiety of the complex **1**.

**TABLE 3: Charge Distribution on Each Atom of the Ion Complex**

atom	interface <sup>a</sup>						in water $\epsilon = 80^b$
	A	B	C	D	E	F	
H1	0.309	0.309	0.306	0.310	0.300	0.299	0.297
N2	-0.369	-0.364	-0.364	-0.363	-0.371	-0.372	-0.372
H3	0.261	0.262	0.263	0.264	0.266	0.266	0.267
C4	0.376	0.379	0.384	0.376	0.387	0.386	0.386
H5	0.262	0.263	0.266	0.265	0.268	0.268	0.269
N6	-0.362	-0.361	-0.360	-0.361	-0.368	-0.370	-0.370
H7	0.307	0.307	0.304	0.308	0.298	0.298	0.295
N8	-0.347	-0.306	-0.349	-0.347	-0.337	-0.336	-0.334
O9	-1.286	-1.278	-1.272	-1.283	-1.268	-1.267	-1.269
P10	2.669	2.668	2.667	2.656	2.665	2.664	2.689
O11	-1.292	-1.284	-1.277	-1.286	-1.271	-1.271	-1.272
O12	-0.783	-0.785	-0.787	-0.784	-0.788	-0.788	-0.797
O13	-0.783	-0.785	-0.787	-0.784	-0.788	-0.788	-0.797
H14	0.265	0.258	0.252	0.260	0.248	0.248	0.245
H15	0.265	0.258	0.262	0.260	0.248	0.248	0.245

<sup>a</sup> The interface position indicated in Figure 2. <sup>b</sup> The dielectric constant of water. <sup>c</sup> Numbering of the atoms is given in Figure 6.

## Discussion

First, we compare comprehensively the results for the ion complex with those for the neutral complex. In the ion complex, the available experimental data are for the binding constant of the **1**–ATP(or AMP) complex at the monolayer–water interface<sup>11,12,17</sup> and for that of its model system, the guanidinium cation and phosphate anion, in aqueous solution.<sup>19</sup> According to those data, the binding constant between the guanidinium and phosphate moieties increases  $10^6$ – $10^7$  times on going from pure water to the monolayer–water interface. The present calculation reproduced well this binding enhancement on the assumption of interface C (Figure 2). On the other hand, it has been reported that the binding constant of the **2**–thymine complex is  $2 \times 10^2 \text{ M}^{-1}$  at the monolayer–water interface, and this value is nearly equal to that for a model system, 1-butylythymidine and pyridinediamide, in chloroform.<sup>18</sup> The calculated binding constant for the neutral complex is  $0.29 \times 10^2 \text{ M}^{-1}$  on the assumption of interface C (Figure 3) and  $1.7 \times 10^2 \text{ M}^{-1}$  in the medium with a dielectric constant of 2, which is somewhat smaller than that of chloroform. Consequently, the calculated results are consistent with both observations of the ion and neutral complexes. We can thus conclude that the double-layer model used here well reproduces the characteristics of the actual monolayer–water interface.

In the present study, such a quantitative comparison of the calculated and observed data for the binding constants does not necessarily have a significant meaning, because the binding energies obtained here were not based on the exact free energies in the dissociated states. Instead, we can show that the above argument is reasonable on the basis of charge distribution analysis.

The results of Mulliken population analysis were summarized in Table 3, where the atomic charge distributions on the reactive site of the ion complex are listed for the cases of the interface positions A–F and for that of the aqueous medium with a dielectric constant of 80. When the interface is placed at A–D, the net charges on O9 and O11 are smaller than the corresponding values in the aqueous medium. This means that these atoms become more electron-rich when the phosphate moiety is located near the interface. When this moiety is fully apart from the the interface (interface E and F), the net charges on these atoms become close to the corresponding values in the aqueous medium. On the other hand, compared with the case of the aqueous medium, H1 and H7 atoms have fewer electrons when the complex is placed on interface A–D. In the cases of

interface E and F, the net charges on these atoms are also close to the corresponding values in the aqueous medium. On the basis of these results, it can be concluded that the O9···H1 and O11···H7 hydrogen bonds are strengthened when the complex is placed on interface A–D, even if the binding sites are exposed to the aqueous phase (interface B, C, and D).

It cannot be directly confirmed whether the above anomalous charge displacements are physically realistic or not. However, we can present a few examples similar to the above case. As described in the introductory remarks, the CD cavity serves as an electrostatic environment capable of catalyzing some reactions of bound guests. In the previous study,<sup>22</sup> we have successfully analyzed the decarboxylation of phenylcyanoacetate anion complexed with CD using a reaction field calculation with a multi-dielectric model similar to Figure 4.

In that calculation, the CD cavity was approximated by a cylinder with a low dielectric constant, a region of which was surrounded by the aqueous medium with a dielectric constant of 80. The substrate was placed on the interface between the cavity and the aqueous medium. It was indicated that the reaction is accelerated even when the reaction center ( $\text{COO}^-$ ) is exposed to the aqueous phase, although decarboxylation is usually accelerated in a low dielectric media. In addition, the reaction rate was quantitatively reproduced by displacing the interface to the electrostatically reasonable position. The acceleration of the reaction was ascribed to the lowering of the transition state. Then, the reaction center of the transition state was shown to become more electron-rich on complexation with CD than that in the aqueous medium. This is quite similar to the charge changes observed for the phosphate moiety on going from the aqueous medium to interface A–D. For several CD–guest complexes, the occurrence of such characteristic charge changes has been experimentally supported by measuring  $^{13}\text{C}$ -NMR chemical shifts of the bound guests.<sup>23</sup>

One of the most important findings in this study is that the hydrogen bond formation is favored on the water side of the interface compared with that in bulk water. This indicates that the nearby lipid phase with the low dielectric constant modulates an electrostatic potential in the neighborhood of the interface and thus contributes to favoring the stabilization of the hydrogen bond.

The presence of such interfacial effects is supported by a recent report based on pure classical electrostatics. Smart and McCammon have represented a docosyl amine monolayer formed at an air–water interface by an electric double layer composed of two dielectrics with dielectric constants of 1 and 78.<sup>29</sup> The titrating head groups of the docosyl amines were placed on or near the air–water interface, and the energies of charged and neutral docosyl amines were evaluated by solving the nonlinear Poisson–Boltzmann equation. According to their results, the  $\text{pK}_a$  of the docosyl amine is lowered  $-0.91$  relative to that in bulk solvent when the nitrogen atoms of the monolayer head groups are displaced  $0.25 \text{ \AA}$  on the water side of the interface. This means that the nearby air phase contributes to favoring a neutral monolayer, consistent with the present results indicating the stabilization of the hydrogen bond.

In the current model, it was assumed that the dielectric constant changes as a step function from 2 to 80. Finally, we discuss the validity of this. Sanders and Schwonek have obtained an empirical function representing the dependence of the dielectric constant on the position along the bilayer normal,<sup>30</sup> based on the population of interfacial water concentration obtained from a neutron scattering study of phosphatidylcholine bilayer.<sup>31</sup> Figure 11a shows the plot of dielectric constants, calculated from this function, on the water side. Certainly, the

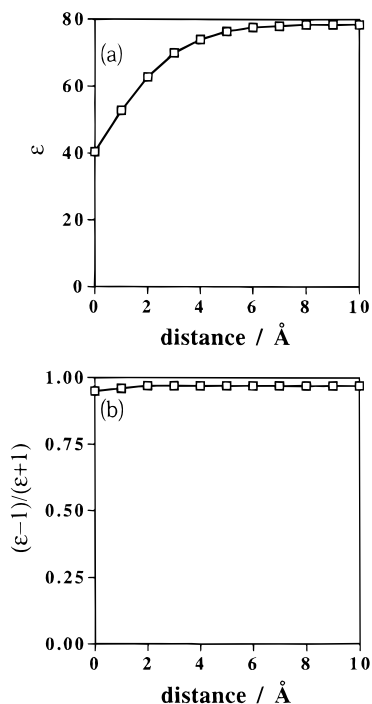


**Figure 11.** Dependence of the dielectric constant ( $\epsilon$ ) and the value of  $(\epsilon - 1)/(\epsilon + 1)$  of water phase on the position along the bilayer normal. (a) Dependence of the dielectric constant ( $\epsilon$ ) of the water phase on the distance from the interfacial region between water and the bilayer. (b) Dependence of the value of  $(\epsilon - 1)/(\epsilon + 1)$  of the water phase on the distance from the interfacial region between water and the bilayer.

dielectric constant changes gradually from 40.25 to 78 in the interfacial region. At a first glance, this seems to be inconsistent with the current model, in which the dielectric constant on the water side is taken to be uniformly 80. However, it should be noted that in general a reaction field is not a linear function against dielectric constant  $\epsilon$ , but approximately depends on  $(\epsilon - 1)/(\epsilon + 1)$ . Figure 11b shows the plot of a reaction field along the bilayer normal, which is calculated from Figure 11a. Clearly, a reaction field is nearly uniform in the vicinity of the interface, supporting the current model. Of course, this is a picture held before the interfacial potential is modified by the presence of the nearby lipid phase. On the other hand, as described above, the experimentally used monolayers of **1** and **2** are solid-like assemblies of these lipids, and hence water molecules could not penetrate into the lipid phase. It is also reasonable to assume that the dielectric constant on the lipid side is uniform. Therefore, the current continuum model can be regarded as a good first-order approximation of the lipid–water interface.

## Conclusion

The continuum model used here well reproduced the experimental facts that the binding energies of hydrogen-bonding systems are amplified at the lipid–water interface compared with those in bulk water. The occurrence of such phenomena was also supported by the results for the charge distribution changes induced by the presence of the interface. Considering the generality of the model, it can be concluded that the enhancement of intermolecular binding is a universal phenomenon which could occur on the water side of an interface formed between a hydrophobic region and water. In other words, the interfacial potential on the water side can be significantly

modified by reaction fields generated from the hydrophobic phase. An analytical solution of the interfacial potential will be described in the next paper.

In conclusion, the current study provides a theoretical background for a conventional strategy to realize molecular recognition through hydrogen bondings. Although the model used here is highly simple, we believe that it is useful as a starting point for the analysis of other interfacial phenomena.

**Acknowledgment.** The authors thank the computer center of the Institute for Molecular Science, Okazaki, Japan, for the use of the super computer NEC SX-3.

## References and Notes

- (1) Huang, C.-Y.; Cabell, L. A.; Anslyn, E. V. *J. Am. Chem. Soc.* **1994**, *116*, 2778–2792.
- (2) Furuta, H.; Magda, D.; Sessler, J. L. *J. Am. Chem. Soc.* **1991**, *113*, 978–985.
- (3) Ikeura, Y.; Kurihara, K.; Kunitake, T. *J. Am. Chem. Soc.* **1991**, *113*, 7342–7350.
- (4) Kimura, E.; Kodama, M.; Yatsunami, T. *J. Am. Chem. Soc.* **1982**, *104*, 3182–3187.
- (5) Rebek, J., Jr.; Askew, B.; Ballester, P.; Buhr, C.; Jones, S.; Nemeth, D.; Williams, K. *J. Am. Chem. Soc.* **1987**, *109*, 5033–5035.
- (6) Hanessian, S.; Gomtsyan, A.; Simard, M.; Roelens, S. *J. Am. Chem. Soc.* **1994**, *116*, 4495–4496.
- (7) Nowick, J. S.; Chen, J. S. *J. Am. Chem. Soc.* **1992**, *114*, 1107–1108.
- (8) Nowick, J. S.; Chen, J. S.; Noronha, G. *J. Am. Chem. Soc.* **1993**, *115*, 7636–7644.
- (9) Nowick, J. S.; Cao, T.; Noronha, G. *J. Am. Chem. Soc.* **1994**, *116*, 3285–3289.
- (10) Bonar-Law, R. P. *J. Am. Chem. Soc.* **1995**, *117*, 12397–12407.
- (11) Sasaki, D. Y.; Kurihara, K.; Kunitake, T. *J. Am. Chem. Soc.* **1991**, *113*, 9685–9686.
- (12) Sasaki, D. Y.; Yanagi, M.; Kurihara, K.; Kunitake, T. *Thin Solid Films* **1992**, *210/211*, 776–779.
- (13) Eliseev, A. V.; Schneider, H. *J. Am. Chem. Soc.* **1994**, *116*, 6081–6088.
- (14) Cha, X.; Ariga, K.; Onda, M.; Kunitake, T. *J. Am. Chem. Soc.* **1995**, *117*, 11833–11838.
- (15) Cha, X.; Ariga, K.; Kunitake, T. *Bull. Chem. Soc. Jpn.* **1996**, *69*, 163–168.
- (16) Cha, X.; Ariga, K.; Kunitake, T. *Chem. Lett.* **1996**, 73.
- (17) Sasaki, D. Y.; Kurihara, K.; Kunitake, T. *J. Am. Chem. Soc.* **1992**, *114*, 10994–10995.
- (18) Kurihara, K.; Ohto, K.; Honda, Y.; Kunitake, T. *J. Am. Chem. Soc.* **1991**, *113*, 5077–5079.
- (19) Springs, B.; Haake, P. *Bioorg. Chem.* **1977**, *6*, 181–190.
- (20) Hoshi, H.; Sakurai, M.; Inoue, Y.; Chujo, R. *J. Chem. Phys.* **1987**, *87*, 1107–1115.
- (21) Hoshi, H.; Sakurai, M.; Inoue, Y.; Chujo, R. *J. Mol. Struct. (THEOCHEM)* **1988**, *180*, 267–281.
- (22) Furuki, T.; Hosokawa, F.; Sakurai, M.; Inoue, Y.; Chujo, R. *J. Am. Chem. Soc.* **1993**, *115*, 2903–2911.
- (23) Sakurai, M.; Hoshi, H.; Inoue, Y.; Chujo, R. *Chem. Phys. Lett.* **1989**, *163*, 217–220.
- (24) Recently, our solvation theory has been developed so as to be able to optimize the geometry of a molecule dissolved in a dielectric continuum. However, it is not easy to apply the optimization method to the heterogeneous medium as shown in Figure 4. Here, in order to treat both cases of homogeneous and heterogeneous continuums with the uniform level of approximation, we used the geometries optimized in vacuo.
- (25) Dewar, M. J. S.; Zoebisch, E. G.; Healg, E. F.; Stewart, J. J. P. *J. Am. Chem. Soc.* **1985**, *107*, 3902–3909.
- (26) Bocker, J.; Schlenkrich, M.; Bopp, P.; Brickmann, J. *J. Phys. Chem.* **1992**, *96*, 9915–9922.
- (27) Tarek, M.; Tobias, D. J.; Klein, M. L. *J. Phys. Chem.* **1995**, *99*, 1393–1402.
- (28) Raghavan, K.; Reddy, M. R.; Berkowitz, M. L. *Langmuir* **1992**, *8*, 233–240.
- (29) Smart, J. L.; McCammon, J. A. *J. Am. Chem. Soc.* **1996**, *118*, 2283–2284.
- (30) Sanders, C. R., II; Schwonek, J. P. *Biophys. J.* **1993**, *65*, 1207–1218.
- (31) Wiener, M. C.; White, S. H. *Biophys. J.* **1992**, *61*, 434–447.